The development of organic spin valves from unipolar to bipolar operation

Tho D. Nguyen, Eitan Ehrenfreund, and Z. Valy Vardeny

We review the first 10 years of research on organic spin-valve devices in the field of organic spintronics. The device figure of merit, magnetoresistance, is governed by the hyperfine interaction of the organic interlayer and the ability of the ferromagnetic electrodes to inject spin-polarized carriers. By choosing a deuterated π-conjugated polymer with a relatively long spin diffusion length as the organic interlayer and using a thin LiF buffer layer to raise the Fermi level of the cathode, a bipolar spin-valve device could be obtained in which the electroluminescence emission intensity is controlled by an external magnetic field. We show that the underlying physics of this spin-organic light-emitting diode is very different from that of a unipolar organic spin valve because of the magnetic properties of the spin-polarized bipolar space charge limited current in the device.

Introduction

A report on magnetoresistance (MR) in a lateral organic diode with ferromagnetic (FM) electrodes in 2002[1] marked the entrance of organics into the well-developed, two-decades old field of spintronics based on the giant MR (GMR) effect in spin valves.[2,3] Subsequently, a demonstration[2] of the first vertical organic spin valve (OSV) device in 2004 (see **Figure 1**) boosted the young field of organic spintronics that propelled many follow-up studies.[3–7] OSV devices, similar to their inorganic analogs, are devices for which the electrical resistance switches between high and low values with the application of relatively small magnetic field. These devices have been based on unipolar injection of charges and passive operation; namely, only one kind of spin-polarized charge (either holes or electrons) was injected and subsequently collected by FM electrodes. Their operation was limited to the control of device resistance upon application of a relatively small magnetic field, $B < 100$ mT.

It was not until 2012 that a truly bipolar OSV was introduced that showed both GMR and hysteretic variations in the device electroluminescence (EL) upon the application of a magnetic field: magnetoelectroluminescence (MEL).[8] The MEL figure of merit is Δ(EL)/EL(%). The operation of such a device, dubbed "spin-organic light-emitting diode" or spin-OLED,[9] was limited to temperatures $T < 200$ K and showed a maximum MEL of ~1%. Nevertheless, it proved that spin alignment of both injected electrons and holes can be obtained in an OLED. The operation of a spin-OLED is similar to that of an ordinary OLED except that the spin polarization of the injected electrons and holes alters the eventual electron-hole radiative recombination, leading to a MEL response that follows the coercive fields of FM electrodes.

The operation of a spin-valve device rests upon the ability of the FM electrodes to efficiently inject and subsequently collect spin-polarized charges and the ability of the interlayer between the electrodes to maintain the injected spin polarization throughout its thickness, d. Therefore, the device interlayer should possess a spin diffusion length, $\lambda_S \sim d$. In organics, where charge hopping is the main electrical conduction mechanism, $\lambda_S = (D\tau_S)^{1/2}$, where D is the charge diffusion coefficient and τ_S is the spin relaxation time. Composed of light elements, organic semiconductors (OSCs) have relatively small spin–orbit interaction. In the absence of spin–orbit interaction, the main spin diffusion length-limiting mechanism in organics is the spin flip caused by the hyperfine interaction (HFI) between the spins of the charge carrier and adjacent nuclei. The small HFI (~3 mT) in OSC leads to a large τ_S ~1–10 μs. However, OSCs have small carrier mobility ($\mu \sim 10^{-7}$–10^{-9} m^2/Vs)[10] leading to D ($= \mu k_B T/e$, where μ is the carrier mobility, k_B is the Boltzmann constant, and e is the elementary charge) ~10^{-9}–10^{-11} m^2/s at room temperature. Thus, λ_S in OSCs is expected

Tho D. Nguyen, Physics and Astronomy Department, University of Georgia, USA; thonguyen08@gmail.com
Eitan Ehrenfreund, Technion-Israel Institute of Technology and University of Utah, USA; eitaneh@gmail.com
Z. Valy Vardeny, Physics and Astronomy Department, University of Utah, USA; valy_vardeny@yahoo.com
DOI: 10.1557/mrs.2014.129

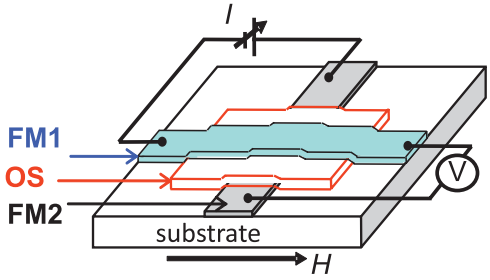

Figure 1. Organic spin-valve architecture. FM1 and FM2 are ferromagnetic electrodes with different coercive fields. OS is the organic interlayer. Under fixed bias (V_b = constant), the current, I, through the device is monitored, while the magnetic field (B) is swept probing both parallel (FM1||FM2) or anti-parallel electrode magnetizations.

to be on the order of 10–100 nm;[11–13] this, in turn, limits the OSV interlayer thickness, $d \sim \lambda_s$.

The operation of the spin-OLED device is determined by spin injection into and diffusion through the active interlayer and also by the dependence of the EL intensity on the electron and hole spin polarization. In general, the EL emission in an OLED is due to a recombination of the injected electrons and holes with spin ½ that are paired in a spin singlet configuration ("singlet exciton," S = 0). Therefore, the singlet exciton density, and consequently the EL intensity, depends on the spin polarization of the injected carriers that result in the MEL having a spin-valve field response. Furthermore, in OLEDs, wherein both EL and longer wavelength electrophosphorescence are substantial, the magnitude of MEL is different from that of magneto-phosphorescence, enabling the modulation of the spin-OLED emission color. This would be quite a feat in organic displays, which are dominated at the present time by OLEDs with non-magnetic electrodes.

One of the major obstacles in realizing a spin-OLED device is the bias voltage needed to generate EL emission. Typical OSV response is limited to low bias voltages (<1 V),[4] whereas for efficient EL in OLEDs, much higher bias is required (>10 V for Alq_3-based OSV, where Alq_3 is aluminum tris-hydroxyquinoline).[4,16–18] In fact, this is one of the main reasons why spin-OLED devices could not be realized until 2012, when a Co/LiF FM electrode was used to reduce the bias voltage needed for bipolar injection.[8] In this review, we briefly discuss the issues of interface spin polarization, spin diffusion through the organic layer, and the operation of spin-OLED.

Spin polarization

A typical vertical OSV structure is shown in Figure 1, where the organic interlayer is placed between the bottom (FM1) and top (FM2) electrodes that have different coercive fields, $B_{c1} \neq B_{c2}$, where B_{c1} is the coercive field for the bottom electrode, and B_{c2} is the coercive field for the top electrode. Originally, metallic Co was used for FM2, whereas the "half metal" $La_{0.67}Sr_{0.33}MnO_3$ (LSMO) was utilized for FM1.[4] LSMO shows nearly 100% spin polarization at cryogenic temperatures; however, its relatively low FM transition temperature ($T_c \sim 307$ K) makes it impractical for use at room temperature.

Interface spin polarization

Spin injection from the metallic FM electrode into the organic layer is in general very inefficient and may be altered by inserting a thin insulating film in between the FM electrode and the OSC layer.[19,20] Indeed, a thin LiF film placed between the top FM electrode (FM2, NiFe alloy) and OSC layer (Alq3) was shown to affect the spin sense of spin-polarized carriers.[15,21] The effect of the LiF buffer layer was to shift the OSC molecular orbital levels with respect to the Fermi energy of the FM contact; such a shift may change the spin sense of the injected carriers.[14]

The requirement for efficient spin injection into the OSC interlayer is even more stringent for a bipolar spin-OLED, since holes and electrons are injected from opposite electrodes, and both need to be spin-polarized. The use of the LiF buffer layer between the cathode and OSC layer is known to allow low-voltage electron injection in the OLED.[22] Therefore, the buffer layer serves to both lower the operating voltage of

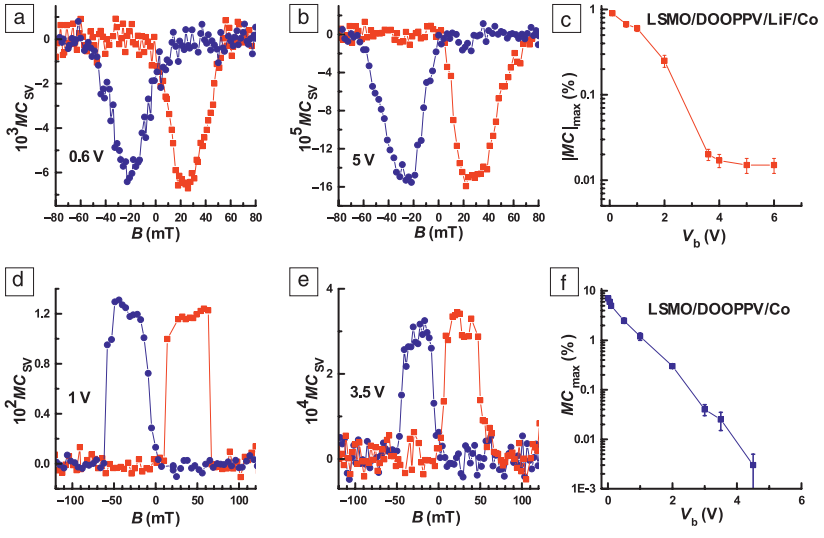

Figure 2. (a–b) Magneto-conductance, $MC(B)$ (≡$-MR(B)$), response of a bipolar organic spin valve (OSV) composed of a LiF covered Co-cathode (thickness d' = 1.5 nm) at two bias voltages, V_b; and (c) summary of the maximum value of MC, denoted MC_{SV}, as a function of bias voltage. (d–f) Same as (a–c) but for a plain Co-cathode ("unipolar" device, d' = 0). The OSV devices were based on $La_{0.67}Sr_{0.33}MnO_3$ (LSMO)/D-DOOPPV(d)/LiF(d')/Co measured at 10 K (thickness d = 25 nm).[10] From these plots, the addition of the LiF layer yields changes in the sign and value of the magnetoconductance. For bipolar organic spin valves, a high bias voltage does not hinder the operation of the device. Red/blue curves representing magnetoresistance measurements made while increasing/decreasing B. Note: B, magnetic field; D-DOOPPV, deuterated-poly(dioctyloxy)phenylvinylene; MR, magnetoresistance; MC_{max}, maximum magnetoconductance.

the OLED and manipulate the spin polarization sense of the injected carriers. Consequently, in spin-OLEDs, the thin LiF buffer layer reduces the turn-on voltage from ~10 to 3.5 V, making it possible to observe the hysteretic MEL response.[8] This is shown in **Figure 2** for an OSV based on deuterated-poly(dioctyloxy)phenylvinylene (D-DOOPPV) as the active interlayer OSC, LSMO as the anode, and Co as the cathode. Comparing Figure 2a–b (LiF/Co cathode, bipolar device) and Figure 2d–e (plain Co cathode, unipolar device), it is clear that the addition of the LiF layer yielded changes in the sign and value of the magnetoconductance (MC). Importantly, while MC is a rapidly decreasing function of the bias voltage for the unipolar device (Figure 2f), it levels off at the start of bipolar injection at V_b~3.5 V (Figure 2c).[8] It implies that, unlike unipolar devices, high bias voltage would not hinder the operation of a bipolar OSV.

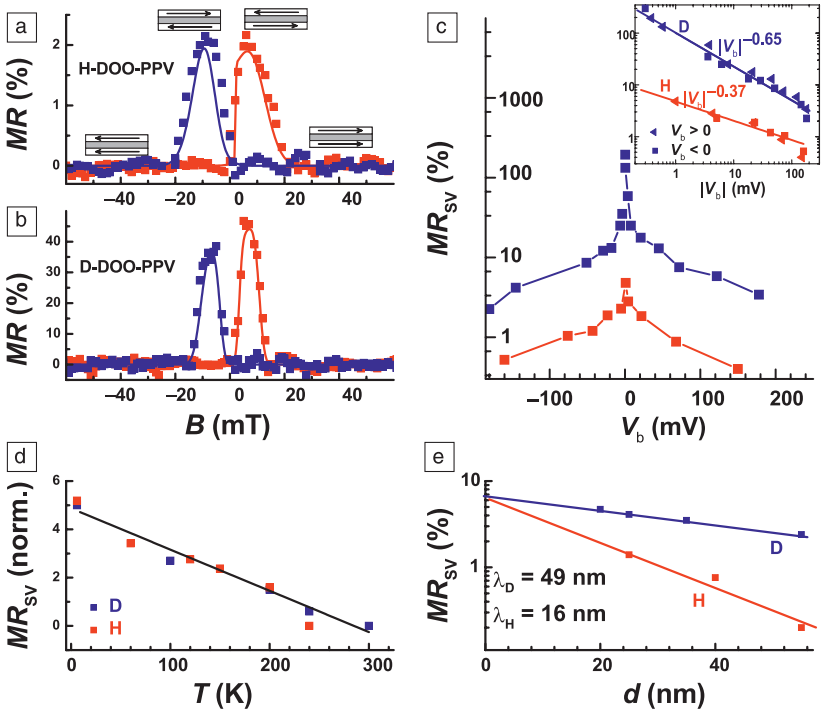

Figure 3. Isotope dependence of magnetoresistance (MR) in organic spin valves (OSVs) based on poly(dioctyloxy)phenylvinylene (DOOPPV).[17] (a–b) MR loop of $La_{0.67}Sr_{0.33}MnO_3$ (200 nm)/DOOPPV (25 nm)/Co (15 nm) spin-valve device measured at temperature T = 10 K and V_b = 10 mV, based on (a) H (π-conjugated)- and (b) D (deuterated)-DOOPPV. The blue (red) curve denotes MR measurements made while decreasing (increasing) the magnetic field, B. The nominal resistance is around ~200 kΩ. The antiparallel and parallel configurations of the FM magnetization orientations are shown in the insets. The data show that the deuterated polymer has superior performance compared to the hydrogenated polymer. (c) The maximum MR value, MR_{SV}, of organic spin valves (OSVs) fabricated in a similar way to those shown in (a–b) (with d_f = 35±5 nm), as a function of V_b measured at T = 10 K. Inset: same data plotted on a log-log scale. The data show that the deuterated polymer is superior to the hydrogenated polymers at all bias voltages. (d) Normalized MR_{SV} of OSVs similar to those shown in (a–c) as a function of temperature measured at V_b = 80 mV. The lack of isotope dependence shows that the MR_{SV} temperature dependence does not originate from the HFI. (e) MR_{SV} of D- and H-polymer OSV (similar to those shown in a–d) of various thicknesses measured at T = 10 K and V_b = 80 mV. The lines are fits to $MR_{SV}(d) = 6.7\% \exp(-d/\lambda_s)$; the fitting parameters are λ_D and λ_H for the two isotopes are marked on the figure. The data show that the deuterated polymer is superior to the hydrogenated polymer as an organic layer in OSV because of its larger spin diffusion length caused by its smaller HFI strength. Note: V_b, bias voltage; d, thickness; λ_S, spin diffusion length; HFI, hyperfine interaction.

Spin diffusion in organic semiconductors

Whereas spin injection involves the OSC/FM interface, maintaining the spin polarization throughout the organic interlayer thickness in the OSV depends solely on the OSC material used. The spin–orbit interaction is very small in an OSC, although non-negligible,[23] and therefore the HFI becomes a major spin flip interaction in these materials. Consequently, it was concluded[17] that if the spin–orbit coupling is indeed weaker than the HFI, then the OSV device performance might be enhanced simply by manipulating the nuclear spins (and consequently also the HFI) of the interlayer OSC using an appropriate isotope exchange. In turn, the isotope exchange also determines the spin relaxation time (via the HFI) that dominates the spin diffusion length in the OSV device.[10,17,24]

The role of the HFI in the OSV response was studied in one case by replacing all strongly coupled hydrogen atoms in the organic π-conjugated polymer DOOPPV interlayer (H-DOOPPV), with deuterium atoms (D-DOOPPV) having a much smaller HFI constant. The H- or D-DOOPPV film was sandwiched between two FM electrodes—LSMO and Co films—with low-temperature coercive fields B_{c1}≈4 mT and B_{c2}≈10 mT. Since $B_{c1} \neq B_{c2}$, it is possible to switch the relative magnetization directions of the FM electrodes from parallel (P) to anti-parallel (AP) alignment (and vice versa) upon sweeping the external magnetic field, B (**Figure 3**a–b), where the device resistance depends on the relative magnetization orientations. According to the original Jullière formula,[25] the maximum MR value, MR_{SV}, is determined by the spin polarization of the FM electrodes, namely P_1 and P_2 via the relation: $MR_{SV} = 2P_1P_2/(1-P_1P_2)$. For materials where λ_S is not infinitely long, a modified formula that takes into account the decay of spin polarization is used:[4,26]

$$MR_{SV} = \frac{2P_1P_2 \exp(-d/\lambda_S)}{1 - P_1P_2 \exp(-d/\lambda_S)} \quad (1)$$

The MR_{SV} value was obtained from the magnetic field dependent resistance, $R(B)$, measurements in OSVs based on the two DOOPPV polymers at various bias voltages, V_b (Figure 3d) and temperatures, T (Figure 3e) using the same LSMO substrate.[17] Figure 3a–b shows representative $MR(B) = [R(B)-R_0]/R_0$ (R_0 is the reference resistance value) hysteresis loops for two similar OSVs (d~25 nm) based on H- and D-DOOPPV at T = 10 K and bias voltage V_b = 10 mV. Importantly, the devices based

on D-DOOPPV showed much larger MR_{SV} values than those based on H-DOOPPV. The improved magnetic properties of OSVs based on D-DOOPPV were explained using Equation 1 assuming a larger λ_S. Indeed, the major difference between the injected spin ½ carriers in D- and H-DOOPPV is their spin relaxation time τ_S, which was shown to be much longer in the D-polymer using optically detected magnetic resonance experiments.[18] Figure 3e shows the $MR(B)$ response of OSVs having various DOOPPV thicknesses (d), but otherwise the same LSMO substrate, which were measured at the same temperature and voltage.[17] From the exponential $MR_{SV}(d)$ dependence, the spin diffusion lengths were obtained:[17] $\lambda_D = 49$ nm, whereas $\lambda_H = 16$ nm, showing that the smaller HFI in D-DOOPPV increases the spin diffusion length λ_S of this polymer.

Hysteretic magneto-electroluminescence in spin-OLED

Using D-DOOPPV as the organic spacer material in order to increase the spin diffusion length, and a LiF buffer layer between the Co film and the OSC layer as the cathode in order to reduce the voltage needed for bipolar injection, a spin-OLED device was fabricated that showed ~1% hysteretic $MEL(B)$ response at low temperatures.[8] The device structure was LSMO/D-DOOPPV(d)/LiF(d') /Co/Al. The turn-on voltage V_o for the EL emission in this device was V_o~3.5 V, compared to V_o~10 V without the LiF layer.

The obtained magneto-electroluminescence $MEL_{EX}(B) \equiv [EL(B)\text{-}EL^{(P)}]/EL^{(P)}$ response (**Figure 4**a, where $EL(B)$ is the measured EL at magnetic field B, and $EL^{(P)}$ is the measured EL for parallel electrode magnetization) of the bipolar OSV is composed of a "non-hysteretic" smooth component, MEL_{nhys}, due to the intrinsic diode response and a "hysteretic" negative component, MEL_{hys}, that consists of a downward sharp dip of ~1% in the antiparallel magnetization configuration between 4 mT and 30 mT, which followed the electrodes' coercive fields. One of the most prominent features of the non-hysteretic response is the very weak dependence of its maximum value, $MEL_{max} \equiv \max(|MEL_{hys}|)$ on the bias voltage V_b (Figure 4c). This response substantially differs from the strong decrease of MR_{SV} with V_b in unipolar OSVs.[4,27–29] It is thus clear that the performance of the bipolar OSV device degrades less with the bias voltage compared to unipolar devices.

The spin-OLED figure-of-merit, MEL_{max}, was measured[10] for various OSC thicknesses, d, and LiF buffer layer thicknesses, d', as shown in Figure 4d. From the MEL response at various values of the thickness d shown in Figure 4d, a finite effective spin diffusion length $\lambda_s \approx 12$ nm was deduced, which is different from $\lambda_s = 45$ nm obtained in unipolar OSV at a small bias voltage based on D-DOOPPV.[18]

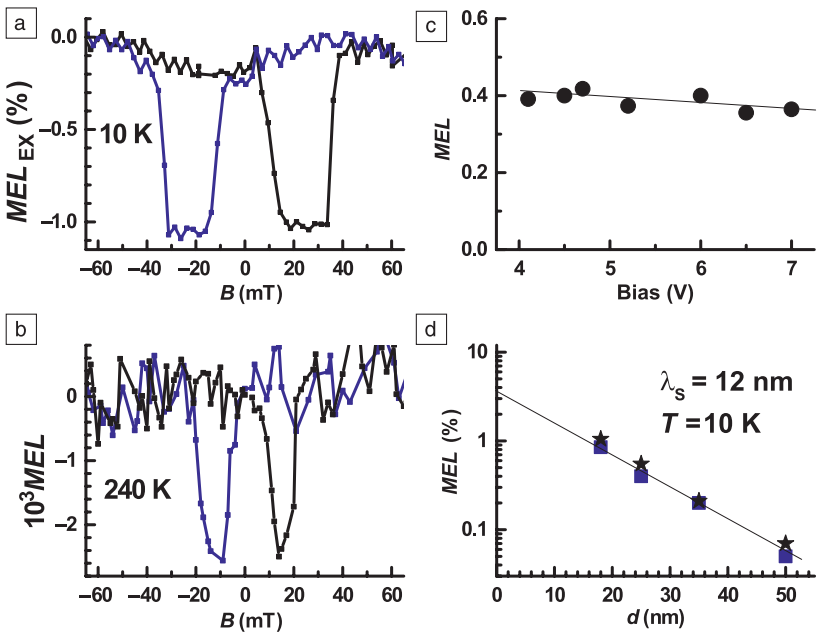

Figure 4. Magneto-electroluminescence (MEL) of a deuterated-poly(dioctyloxy) phenylvinylene spin-OLED (organic light emitting diode) device.[10] (a) As obtained $MEL_{EX}(B)$ response for upward (black) and downward (blue) B-sweeps (B is the magnetic field), measured at bias voltage $V_b = 4.5$ V and temperature $T = 10$ K, for a device thickness of $d = 18$ nm, and a LiF thickness of $d' = 0.8$ nm. The dip in the $MEL(B)$ response is due to spin aligned electrons and holes that are injected from the FM electrodes. (b) The hysteretic $MEL(B)$ response of the same device at 240 K. The narrower $MEL(B)$ response at higher temperature shows that the MEL is a genuine effect rather than an artifact, since the values of the coercive field of the ferromagnetic electrodes decrease at higher temperature. (c) The bias voltage dependence of the maximum, MEL_{SV}, value measured at 10 K. This shows that the MEL in the bipolar device is less dependent on the bias voltage as compared to the magnetoconductance of the unipolar organic spin valve (OSV). (d) The maximum MEL_{SV} response of spin-OLEDs at various thicknesses and LiF buffer layer thickness, $d' = 0.8$ and 1.5 nm (blue, black symbols, respectively), measured at $T = 10$ K and $V_b = 4.5$ volt. The line through the data points represents a fit using Equation 1. This shows that the spin diffusion length of the deuterated polymer in bipolar OSV (~12 nm) is much smaller than that in unipolar OSV devices (~40 nm). Note: $MEL_{EX}(B)$, magneto-electroluminescence; λ_S, spin diffusion length.

Summary

We reviewed the development of the organic spin-valve device during the first decade of focused research in the field of organic spintronics. The device's magnetoresistance is determined by the spin diffusion length in the organic interlayer and spin polarization degree of the ferromagnetic electrodes. This explains the steep decrease in the device performance with the temperature and organic interlayer thickness. Following intensive research, a bipolar organic spin valve was demonstrated, where both spin polarized electrons and holes are injected from the opposite ferromagnetic electrodes. The bipolar spin valve shows ~1% magneto-electroluminescence and indicates that a spin-polarized space charge-limited current occurs in the organic active layer above a threshold bias voltage. The next milestone in this field would be to achieve substantive magnetoluminescence at room temperature.

Acknowledgments

Supported by DOE Grant No. DE-FG02–04ER46109 (isotope exchange; T.D.N. and Z.V.V.), NSF grant No. DMR-1104495 and MRSEC, DMR-1121252 program at the UoU (bipolar OSV; T.D.N. and Z.V.V.), Israel Science Foundation Grant No. ISF 472/11 (bipolar SCLC model; E.E.), and the US-Israel BSF Grant No. 2010135 (spin-OLED; Z.V.V. and E.E.).

References

1. V. Dediu, M. Murgia, F.C. Matacotta, C. Taliani, S. Barbanera, *Solid State Commun.* **122**, 181 (2002).
2. M.N. Baibich, J.M. Broto, A. Fert, F.N. Van Dau, F. Petroff, P. Etienne, G. Creuzet, A. Friederich, J. Chazelas, *Phys. Rev. Lett.* **61** (21), 2472 (1988).
3. G. Binasch, P. Grünberg, F. Saurenbach, W. Zinn, *Phys. Rev. B: Condens. Matter* **39** (7), 4828 (1989).
4. Z.H. Xiong, D. Wu, Z.V. Vardeny, J. Shi, *Nature* **427**, 821 (2004).
5. F.J. Wang, Z.H. Xiong, D. Wu, J. Shi, Z.V. Vardeny, *Synth. Met.* **155** (1), 172 (2005).
6. S. Pramanik, S. Bandyopadhyay, K. Garre, M. Cahay, *Phys. Rev. B: Condens. Matter* **74**, 235329 (2006).
7. S. Majumdar, R. Laiho, P. Laukkanen, I.J. Vayrynen, H.S. Majumdar, R. Osterbacka, *Appl. Phys. Lett.* **89** (12), 122114 (2006).
8. F.J. Wang, C.G. Yang, Z.V. Vardeny, X.G. Li, *Phys. Rev. B: Condens. Matter* **75**, 245324 (2007).
9. T.S. Santos, J.S. Lee, P. Migdal, I.C. Lekshmi, B. Satpati, J.S. Moodera, *Phys. Rev. Lett.* **98**, 016601 (2007).
10. T.D. Nguyen, E. Ehrenfreund, Z.V. Vardeny, *Science* **337**, 204 (2012).
11. V.A. Dediu, L.E. Hueso, I. Bergenti, C. Taliani, *Nat. Mater.* **8**, 707 (2009).
12. H.C.F. Martens, P.W.M. Blom, H.F.M. Schoo, *Phys. Rev. B: Condens. Matter* **61**, 7489 (2000).
13. S. Pramanik, C.-G. Stefanita, S. Patibandla, S. Bandyopadhyay, K. Garre, N. Harth, M. Cahay, *Nat. Nanotechnol.* **2**, 216 (2007).
14. J.H. Shim, K.V. Raman, Y.J. Park, T.S. Santos, G.X. Miao, B. Satpati, J.S. Moodera, *Phys. Rev. Lett.* **100**, 226603 (2008).
15. A.J. Drew, J. Hoppler, L. Schulz, F.L. Pratt, P. Desai, P. Shakya, T. Kreouzis, W.P. Gillin, A. Suter, N.A. Morley, V.K. Malik, A. Dubroka, K.W. Kim, H. Bouyanfif, F. Bourqui, C. Bernhard, R. Scheuermann, G.J. Nieuwenhuys, T. Prokscha, E. Morenzoni, *Nat. Mater.* **8** (2), 109 (2009).
16. I. Bergenti, V. Dediu, E. Arisi, T. Mertelj, M. Murgia, A. Riminucci, G. Ruani, M. Solzi, C. Taliani, *Org. Electron.* **5**, 309 (2004).
17. T.D. Nguyen, G. Hukic-Markosian, F.J. Wang, L. Wojcik, X.G. Li, E. Ehrenfreund, Z.V. Vardeny, *Nat. Mater.* **9**, 345 (2010).
18. R. Lin, F. Wang, J. Rybicki, M. Wohlgenannt, K.A. Hutchinson, *Phys. Rev. B: Condens. Matter* **81**, 195214 (2010).
19. D.L. Smith, R.N. Silver, *Phys. Rev. B: Condens. Matter* **64**, 045323 (2001).
20. P.P. Ruden, D.L. Smith, *J. Appl. Phys.* **95**, 4898 (2004).
21. L. Schulz, L. Nuccio, M. Willis, P. Desai, P. Shakya, T. Kreouzis, V.K. Malik, C. Bernhard, F.L. Pratt, N.A. Morley, A. Suter, G.J. Nieuwenhuys, T. Prokscha, E. Morenzoni, W.P. Gillin, A.J. Drew, *Nat. Mater.* **10** (1), 39 (2011).
22. T.M. Brown, R.H. Friend, I.S. Millard, D.J. Lacey, J.H. Burroughes, F. Cacially, *Appl. Phys. Lett.* **77**, 3096 (2000).
23. S. Bandyopadhyay, *Phys. Rev. B: Condens. Matter* **81**, 153202 (2010).
24. T.D. Nguyen, F. Wang, X.-G. Li, E. Ehrenfreund, Z.V. Vardeny, *Phys. Rev. B: Condens. Matter* **87**, 075205 (2013).
25. M. Julliere, *Phys. Lett. A* **54** (3), 225 (1975).
26. E. Ehrenfreund, Z.V. Vardeny, *Phys. Chem. Chem. Phys.* **15**, 7967 (2013).
27. H. Vinzelberg, J. Schumann, D. Elefant, R.B. Gangineni, J. Thomas, B. Büchner, *J. Appl. Phys.* **103**, 093720 (2008).
28. J.-W. Yoo, H.W. Jang, V.N. Prigodin, C. Kao, C.B. Eom, A.J. Epstein, *Phys. Rev. B: Condens. Matter* **80**, 205207 (2009).
29. T.D. Nguyen, G. Hukic-Markosian, F. Wang, X.-G. Li, E. Ehrenfreund, Z.V. Vardeny, *Synth. Met.* **161**, 598 (2011). □